CHINESE JOURNAL OF MECHANICAL ENGINEERING
Vol. 28, No. 6, 2015

DOI: 10.3901/CJME.2015.0723.100, available online at www.springerlink.com; www.cjmenet.com; www.cjme.com.cn

Springback Prediction and Optimization of Variable Stretch Force Trajectory in Three-dimensional Stretch Bending Process

TENG Fei[1, 2], ZHANG Wanxi[1, 2], LIANG Jicai[1, 2, *], and GAO Song[1, 2]

1 *State Key Laboratory of Structural Analysis for Industrial Equipment, Dalian University of Technology, Dalian 116024, China*

2 *School of Automotive Engineering, Dalian University of Technology, Dalian 116024, China*

Received July 11, 2014; revised April 13, 2015; accepted July 23, 2015

Abstract: Most of the existing studies use constant force to reduce springback while researching stretch force. However, variable stretch force can reduce springback more efficiently. The current research on springback prediction in stretch bending forming mainly focuses on artificial neural networks combined with the finite element simulation. There is a lack of springback prediction by support vector regression (SVR). In this paper, SVR is applied to predict springback in the three-dimensional stretch bending forming process, and variable stretch force trajectory is optimized. Six parameters of variable stretch force trajectory are chosen as the input parameters of the SVR model. Sixty experiments generated by design of experiments (DOE) are carried out to train and test the SVR model. The experimental results confirm that the accuracy of the SVR model is higher than that of artificial neural networks. Based on this model, an optimization algorithm of variable stretch force trajectory using particle swarm optimization (PSO) is proposed. The springback amount is used as the objective function. Changes of local thickness are applied as the criterion of forming constraints. The objection and constraints are formulated by response surface models. The precision of response surface models is examined. Six different stretch force trajectories are employed to certify springback reduction in the optimum stretch force trajectory, which can efficiently reduce springback. This research proposes a new method of springback prediction using SVR and optimizes variable stretch force trajectory to reduce springback.

Keywords: springback prediction, support vector regression (SVR), response surface, particle swarm optimization (PSO)

1 Introduction

Aluminum profile stretch bending forming is widely employed in the production of structural components for cars and high-speed rails. The stretch forming process involves a combination of elasto-plastic stretching and bending deformation of profiles. Elastoplasticity can result in a significant amount of springback after loading in stretch bending forming. Springback can cause twisting, wrinkling, shape errors and assembly difficulties[1–2]. The shape error resulted from springback in the profile stretch bending forming process is seen as a manufacturing defect which must be reduced as much as possible[3–4]. Reducing and predicting springback is still a major challenge in the stretch bending forming process.

Many studies concerning springback have been performed. There are numerous factors that influence springback, such as material parameters, geometric parameters, stretch force trajectories and processing speed[5–10]. CLAUSEN, et al[11], argued that the main factors influencing springback were tensile force and strain hardening properties. After an investigation into the effects of processing parameters on dimensional precision, YU, et al[12], found that springback decreased with the increase of the stretch force. LIANG, et al[13], proposed that an optimized combination of pre-stretch and post-stretch amount could reduce springback. These studies showed that adjusting and optimizing stretch force trajectories in stretch bending forming process could decrease springback. Existing studies that focus on using stretch force to reduce springback mostly apply constant force. Various papers are concentrated on springback reduction. LEE, et al[14], have concluded that smaller clamping force with an increase in die radius of curvature leads to greater springback. OUAKDI, et al[15], showed through tests of aluminum alloy the gradual decrease of springback with the increase of stretching depth. CAO, et al[16], proposed a stepped binder force trajectory algorithm by neural network controller. KITAYAMA, et al[17–18], carried out an optimization method of variable holder force trajectory for springback reduction using sequential approximate optimization with radial basis function network. It was found in that paper that the optimal variable blank hold force trajectory could

* Corresponding author. E-mail: tengfei325@126.com
Supported by National Technical Innovation Foundation of China (Grant No. Jilin Province 350)

drastically reduce springback in comparison with various blank hold force trajectories. The optimal stretch bending was valid for springback reduction. However, there is a lack of optimized stretch force in stretch bending forming process in the past research.

KAZAN, et al[19], proposed a springback predictive model by neural network in the wipe bending process grounded on the data obtained from finite element analysis(FEA). SONG, et al[20], developed a springback predictive model in the T-section beam bending process based on artificial neural networks (ANN) approach, in which the effect of material properties on springback was investigated by numerical simulations using the finite element method. From these papers, it can be conclude that neural networks associated with the finite element method have a wide range of applications in springback prediction. However, few studies have reported that the accuracy of neural networks associated with the finite element method can be ensured. The accuracy of SVM is higher than neural networks. Support vector regression (SVR) is applied in various fields for its generalization ability which is better than that of neural networks. SVR is a regression technique of support vector machines. A SVR model was studied by HONG, et al[21] to examine the feasibility of the reliability prediction model. SINGH, et al[22], predicted the thickness along the cup wall in hydromechanical deep drawing via SVR. This paper indicates that SVR has higher thickness prediction precision than ANN.

The main objective of this work is to predict springback and reduce springback using optimized stretch force trajectories in the three-dimensional stretch bending forming process. The flexible three-dimensional stretch bending die is introduced. The springback prediction model in three-dimensional stretch bending is developed using SVR. The data used for training and testing the SVR model are derived from the experiments. The precision of the SVR model is compared with that of ANN. In order to optimize the stretch force trajectories, the stepped variable stretch forces, pre-stretching elongation and post-stretching elongation are considered as the design variables. Stretch force trajectories are optimized by particle swarm optimization(PSO). The objection and constraints are formulated by response surface. The precision of response surface models is examined. It has been proved that the optimized stretch force trajectory is more effective for reduction of springback.

2 Three-dimensional Stretch Bending Forming Process

2.1 Flexible die

In the flexible stretch-bending forming processes, reconfigurable dies which have several unit bodies are used as forming tools instead of one-shot milled solid dies as shown in Fig. 1. The flexible die generates numerous discrete forming surfaces by changing the head of multi-point die and adjusting the placement of the head of multi-point die according to objective surface. Each unit-body installed in an independent support is composed of a support, a forming slider, a guide sliding block, a vertical guide rail, a limit block and other parts shown in Fig. 2. Screw of height control can control the height of the unit-body. Vertical pin contacting with the screw of height control decides the height of head of multi-point die. Horizontal pin is connected with the unit-body and head of multi-point die. Bolt is linked to the unit-body and stretch bending machine. Bracket supports the parts of unit-body. Guide key guides the unit-body to move along the plate of the stretch bending machine. The connected part and the head of multi-point die could move on vertical rails. Forming plate slider supports the head of multi-point. Guide slider limits the adjustment of the head of multi-point die. Head of the multi-point die is decided by the forming profile. Liner limits the downward movement.

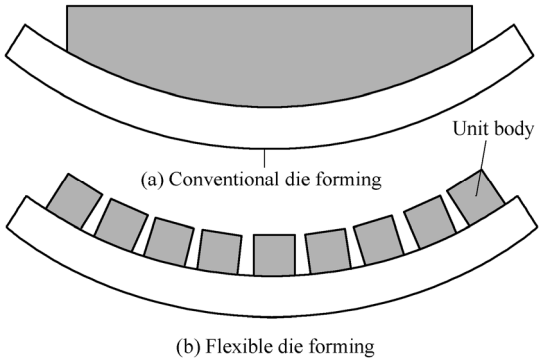

Fig. 1. Schematic view of conventional die forming and flexible forming die

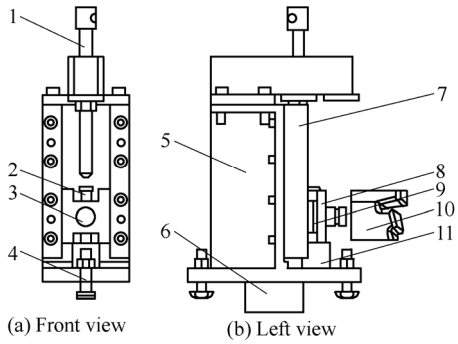

Fig. 2. Diagram of the unit-body

1. Screw of height control; 2. Vertical pin; 3. Horizontal pin; 4. Bolt; 5. Bracket; 6. Guide key; 7. Vertical rails; 8. Forming plate slider; 9. Guided slider; 10. Multi-point die; 11. Liner

2.2 Flexible three-dimensional stretch bending

The most common way of the stretch bending forming process is divided into three stages. In the first stage, the profile bears the stress by applying an axial tensile force called pre-stretching tension at the centroid of the cross-section of profile. In the second stage referred to as bending, the profile is imposed bending moments to be close to the die. In the third stage, the profile is applied axial force called post-stretching force. The three-dimensional

stretch bending forming process means the stretch bending forming in two perpendicular planes. In three-dimensional stretch bending process, the profile is firstly stretched and bended in the horizontal plane and then in the vertical plane. Because the bending forming of three-dimensional stretch is partitioned into two steps bent in the horizontal plane and then in the vertical plane, the three-dimensional stretch bending process is composed of four steps.

2.3 Adjustment calculation method of multi-point die

The values of target shape S, radius R and bending angle θ are available. The distance between the two adjacent unit-bodies is d which can be measured. T-profiles plane is set to the XY plane of the three-dimensional coordinate system, where a unit-body is set to the positive Z-axis direction. The total number of unit-bodies is n, and the number of each unit-body is 1, 2,⋯, i,⋯, n, respectively. The adjustment y_i calculation method of the ith unit-body is shown in Fig. 3. According to the geometric relationships, y_i can be calculated, as given in Eq. (1):

$$y_i^2 = \left[2R\sin\frac{(i-1)\theta}{n-1}\right]^2 - (i-1)d. \tag{1}$$

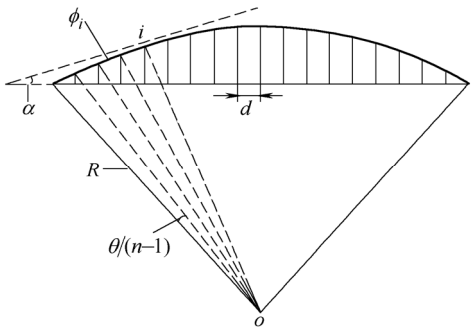

Fig. 3. Calculation of displacement and rotation angle

To constitute the die-face, the sliders need to be rotated. The rotation angle in the XY plane of the slider number i is ϕ_i. From Fig. 3, it can be obtained that when the value ϕ_i is positive, the rotation is clockwise; when the value is negative, the rotation is counterclockwise. The calculation method of rotation angle is given in Eq. (2):

$$\phi_{ij} = \theta - \frac{2(i-1)\theta}{n-1}. \tag{2}$$

Because bending in the vertical plane is the same as that in the horizontal plane, the calculation method of displacement and rotation angle of the slider is the same as the above method.

3 SVR Model and Springback Prediction

3.1 Springback evaluation

There are three common methods to evaluate springback: the variation of curvature radius, the springback angle, the springback displacement of the end of profile, as shown in Fig. 4. Because bending in the vertical plane is the same as that in the horizontal plane, the calculation method of displacement and rotation angle of the slider is the same. This paper sets springback displacement as springback evaluation.

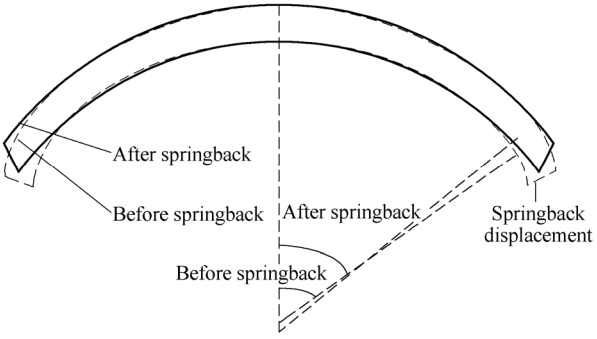

Fig. 4. Springback evaluation

3.2 SVR

Support vector machine (SVM) is a new machine learning method based on statistical theory, and the principle of minimization of structural risk. Nonlinear problems in the original space are mapped into linear problems in high-dimensional feature space by kernel function in SVM[23]. The linear problem works out in this high-dimensional feature space. SVM is mainly used to resolve nonlinear problems. When SVM is used to solve regression problems, it is called support vector regression (SVR). SVR has good performance when the sample number is small. The purpose of SVR is to look for a decision function, such as $y = < w \bullet x > + b$. The procedure of nonlinear regression is described as follows.

(1) For a given training set

$$T = \{(x_1, y_1), \cdots, (x_i, y_i)\} \in (R^n \times Y)^1,$$
$$x_i \in R^n, y_i \in R, i = 1, \cdots, l. \tag{3}$$

In order to infer the corresponding output y to arbitrary x by $y=g(x)$, it is necessary to look for a real-valued function $g(x) \in R$ as per Eq. (3). This problem is a regression problem of R^n in n dimensional space. It can be subdivided into linear and nonlinear regression problems. Regression of springback prediction in three-stretch bending forming process is nonlinear regression problems.

(2) Choosing appropriate kernel function $K(x, x_i)$ and proper positive number ε and penalization parameter C. The commonly used kernel functions are polynomial kernel function and Gaussian radial basis kernel function.

Polynomial kernel function is:

$$K(x, y) = [(x \bullet y) + 1]^d. \tag{4}$$

Gaussian radial basis kernel function is

$$K(x, x_i) = \exp\left(-\frac{\|x - x_i\|^2}{2a^2}\right). \quad (5)$$

(3) Constructing and solving the quadratic programming problems as follows:

$$\min_{\alpha^{(*)} \in R^{2l}} \frac{1}{2}\sum_{i,j=1}^{l}(\alpha_i^* - \alpha_i)(\alpha_j^* - \alpha_j)K(x_i, x_j) + \varepsilon\sum_{i=1}^{l}(\alpha_i^* + \alpha_i) - \sum_{i=1}^{l} y_i(\alpha_i^* - \alpha_i),$$

$$\text{s.t.} \quad \sum_{i=l}^{l}(\alpha_i - \alpha_i^*) = 0,$$

$$0 \leqslant \alpha_i, \alpha_i^* \leqslant \frac{c}{l}, i = 1, 2, \cdots, l. \quad (6)$$

The solution of this problem can be expressed as:

$$\bar{\alpha}^* = \left(\bar{\alpha}_1, \bar{\alpha}_1^*, \cdots, \bar{\alpha}_l, \bar{\alpha}_l^*\right).$$

Constructing the decision function:

$$f(x) = \sum_{i=l}^{l}(\bar{\alpha}_i^* - \bar{\alpha}_i)K(x_i, y_j) + b, \quad (7)$$

where the bias constant b is

$$b = y_j - \sum_{i=1}^{l}(\bar{\alpha}_i^* - \bar{\alpha}_i)K(x_i, x_j) + \varepsilon,\ \bar{\alpha}_j \in \left(0, \frac{C}{l}\right), \quad (8)$$

$$b = y_k - \sum_{i=l}^{l}(\bar{\alpha}_i^* - \bar{\alpha}_i)K(x_i, x_k) - \varepsilon,\ \bar{\alpha}_k \in \left(0, \frac{C}{l}\right). \quad (9)$$

3.3 Design variables

In three-dimensional stretch bending process, pre-stretching that guarantees the straightening of profile makes the stress in axial cross section linearly distributed. The stress difference between outer material σ_o and inner material σ_i could decrease springback. Under the axial pre-stretching force, the stress of the cross section is uniformly distributed, which is $\sigma_{o1}=\sigma_{i1}=\sigma_{0.2}$. $\sigma_{0.2}$ is the yield limit. After the bending process, the stretch stress of outer layer material increases to σ_{o2} along the actual stress curve. However, the stretch stress of inner layer material reduces to σ_{i2} along the actual stress curve. After the post-stretching process, the stretch stress of outer layer material continues to increase to σ_{o3} along the actual stress curve. The stretch stress of inner layer material increases to σ_{i3} until it reaches yield limit $\sigma_{0.2}$ along the actual stress curve. The stress distribution in the center of cross section is shown in Fig. 5.

In order to determine the total axial stretch force, the effect of friction must be considered. The length of the cross section where the curvature radius is the minimum value is divided into j regions as shown in Fig. 6. When considering the friction effect, the total stretch force is P:

$$P = p_{\min}\exp(\mu\alpha_1)\exp(\mu\alpha_2)\cdots\exp(\mu\alpha_j) = p_{\min}\exp(\mu\sum_{i=1}^{j}\alpha_i), \quad (10)$$

$$P_{\min} = S\sigma_{0.2} + \frac{D}{2R_S}\left[H(2S - t_1H) + t(t_1 - B)\right], \quad (11)$$

where S is the area of cross section, D is stress modulus decided by material properties.

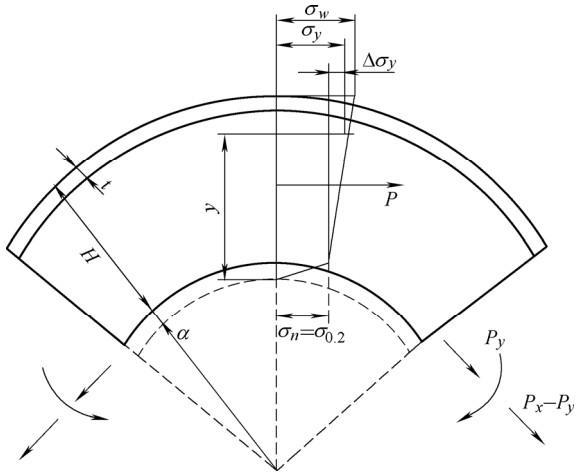

Fig. 5. Stress distribution in the center of cross section

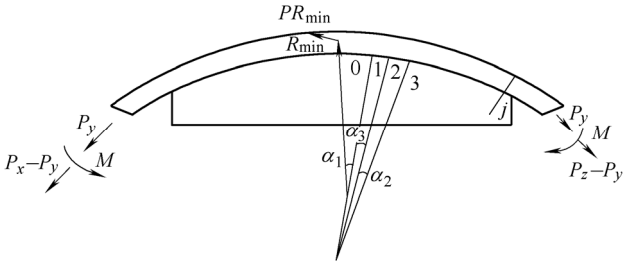

Fig. 6. Expression of the total stretch force

The three stretch bending is partitioned into four steps. Then, the stretch force of each step is taken as the design variable. An illustrative example of the design variables is shown in Fig. 7. There is an obvious effect of pre-stretching elongation and post-stretching elongation on reduction, so they are chosen as the design variables. There are six design variables in the three-dimensional stretch bending process. P_0 is the total stretch force in experiments:

$$P_0 = \sum_{i=1}^{4} x_i. \quad (12)$$

3.4 Experimental setup

The experiments were carried out on the flexible stretch bending machine as displayed in Fig. 8. The profiles in the tests were strictly selected from the same stock to ensure

that the materials were all aluminum AA6082T5. The material parameters of AA6082T5 are as follows: Elasticity modulus E=65 050 MPa, Poisson ratio ν=0.34, Yield stress σ_0=288.2 MPa, Anisotropic parameter of Barlat criterion r_{00}=0.514 r_{45}=0.844 r_{90}=0.626. The dimensions of the aluminum profile section are in Fig. 9. The initial samples were automatically generated by the popular design of experiments (DOE) method. According to the DOE method, sixty experiments were designed and carried out under different combinations of design variables. The lower and upper bounders of the variables were determined by experiments and experience enumerated in the constraint design section. The samples of design space should be sparsely distributed to avoid long-time consuming procedures of forward problems. The experiment results will be utilized to train and test samples of the SVR and ANN models.

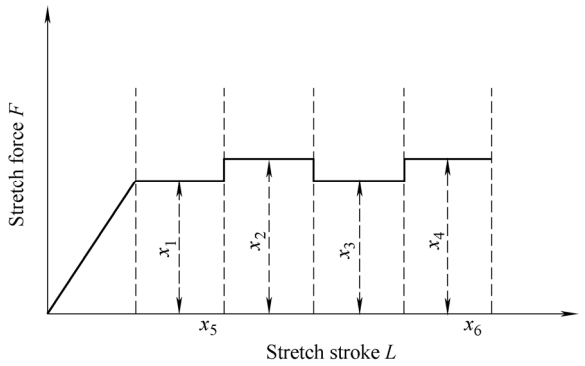

Fig. 7. An example of design variables

Fig. 8. Profile in three-dimensional stretch bending forming process

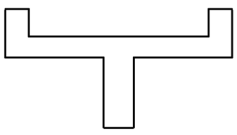

Fig. 9. Geometrical shape of T profile

3.5 Springback prediction

3.5.1 Training of SVR

The springback prediction based on SVR was trained by 40 sets of input-output pairs. In this article, the six design variables were set as input parameters, while the springback displacement and thickness variation were set as output parameters. The different characteristics of the input values were vastly different in size. The training and testing data shall be normalized, since normalization can effectively improve the prediction accuracy and avoid attributes of the values in greater numeric ranges. It can dominate those values in smaller numeric ranges. The training and testing data were normalized to [−1, 1].

The selection of kernel function has great effects on prediction accuracy. The libsvm-3.17 toolbox was used, which was developed by Taiwan University. SVR was divided to epsilon-SVR and nu-SVR. There are three types of kernel functions: linear, polynomial and radial basis function (RBF). In order to find the best combination of SVR class and kernel function, the combinations of these values were researched with results in Table 1. The research trail shows that using the epsilon-SVR and RBF kernel function in the model of springback prediction in stretch bending of profile can obtain higher accuracy.

Table 1. Research of combination of SVR class and kernel function

SVR	Kernel function	Iterations k	Mean squared error σ	Squared correlation coefficient r
Epsilon-SVR	Linear	152	0.132	0.735
Epsilon-SVR	Polynomial	35	0.351	0.204
Epsilon-SVR	RBF	2063	0.093	0.749
Nu-SVR	Linear	64	0.224	0.643
Nu-SVR	Polynomial	30	0.312	0.309
Nu-SVR	RBF	186	0.189	0.521

The parameters required to be determined were C and g, which controlled the tradeoff between model fitting and prediction accuracy. Cross-validation was used to find the best combination of C and g. The choice of parameters of C and g had large impacts on the prediction accuracy of the model. Cross-validation can be used to find the best combination. Various values of C and g were tried and the best-validation accuracy can be picked out. In this paper, grid regression function was used to search the best C and g. According to the trail, the best C=512, g=1, and the mean squared error was 0.032 41. The SVR model was trained by 40 trail samples which were randomly selected from 60 experiment samples.

3.5.2 Testing of SVR

The SVR prediction model was tested by the rest of the trail samples. In order to verify the prediction accuracy, the prediction model of ANN was studied. The training and testing procedure of artificial neural networks was programmed by the NN toolbox of Matlab. There were three layers of network structures in neural networks, encompassing input, hidden and output layers. There were 56 nodes in the hidden layer, and 2 nodes in the output

layer. The model was trained by the data which were used to train SVR model. The training error was controlled within 10^{-5}. The input and output parameters were the same as the model of SVR. Result comparisons of SVR and ANN were shown in Fig. 10. Prediction models of SVR and ANN were evaluated and compared against each other in springback displacement. From the comparison of the fitting with the initial data and the mean squared error, it was proved that SVR had higher accuracy than ANN. From Fig. 10, the results of SVR are more closed to the original data compared to that of ANN, and so the prediction accuracy of SVR is higher.

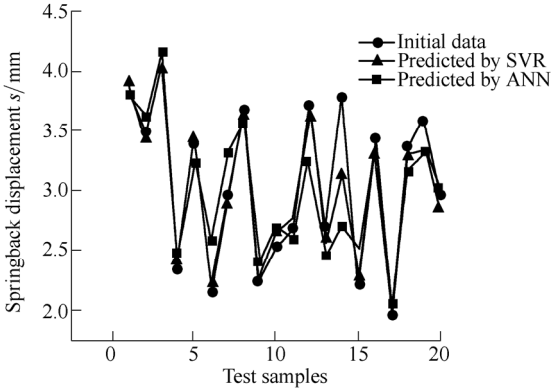

Fig. 10. Comparison of springback prediction using SVR and ANN

4 Optimization of Stretch Force Jrajcetory

4.1 Definition of objective functions

In this section, objective functions of profile three-dimensional stretch bending forming optimization are introduced. The objective function of stretch bending forming problem is based on the springback after unloading:

$$\begin{gathered}\text{Min } S(x),\\ a \leqslant x_i \leqslant b, i=1,2,3,4,\\ c \leqslant x_j \leqslant d,\ j=5,6,\\ p \leqslant g_k(x) \leqslant P, k=1,2,\cdots,n_{\text{con}}.\end{gathered} \tag{13}$$

where $S(x)$ represents the minimized objective function; x denotes the design variables shown in Fig. 8; a and b represent the lower and upper bounds of the ith design variable, respectively; c and d represent the lower and upper bounds of the jth design variable, respectively; $g_k(x)$ denotes the kth constraint, and n_{con} represents the number of constraints.

The investigate operation was characterized by conflicting performances and its optimization can be formulated as an optimization problem.

4.2 Formulation of design optimization problems

The response surface method is one of the most prevalent and simplest surrogate models. The response surface method uses a simple approximation function to replace the actual complex simulation model for easy analysis and calculation. The principle of response surface method is: when the actual function values of the points around a certain point are known, a hypersurface can be set up in some ways. The surface can substitute an actual function for complex calculation in the region which is sufficiently close to the area of the point. X is n dimensional input variable set, and Y is output variable set. In accordance with the experimental data, there is a relationship $K(x)$ between input and output variables. $K(x)$ is the response surface model.

There are four commonly used response surface modeling approaches as follows: polynomial regression, artificial neural networks, Kriging function and radial basis function. The accuracy and efficiency of fitting are important standards to evaluate the response surface modeling method. Springback research in three-dimensional stretch bending is a complicated nonlinear problem. For the polynomial regression method, the second order polynomial is used widely. Second-order polynomial has insufficient description ability to higher-order nonlinear problem. High dimensional polynomial fitting precision causes decreasing fitting precision because of Runges phenomenon. Hence, the polynomial regression method is not suitable for springback research in three-dimensional stretch bending. Although the fitting accuracy of neural network algorithm is high, its computation efficiency is low. And it is easy to fall into local extremum, thereby leading to difficult convergence. The estimation parameter of the Kriging function method is complicated when the input variable is high dimensional. The radial basis function is suitable for high dimensional nonlinear problems. Radial basis function is chosen to fit the springback and optimize the forming parameters in this paper.

The analytical expression for the radial basis function is

$$y(X)=\sum_{i=1}^{m}\lambda_i\phi(r_i, c), \tag{14}$$

where $r_i(X)$ is the distance between the sampling point i and X in design space, ϕ is primary function, c is nonnegative constant, λ is weighting coefficient. In general, any function can be expressed as a set of weighted basis functions, so a nonlinear mapping is from the input samples to the output basis function. The Gaussian function was chosen as the basis function in this paper. Because the value of the Gaussian function only relates to the Euclidean distance between the input point and the center point and the width of the Gaussian function, the fitting function based on the Gaussian function.

After the model of response surface is established, the accuracy should be assessed. The error evaluation indicators of response surface are relative average absolute error (RAAE), determination coefficient R^2, and relative maximum absolute error (RMAE).

$$\mathrm{RAAE}=\frac{\sum_{i=1}^{k}|y_i-\hat{y}_i|}{\sum_{i=1}^{k}|y_i-\overline{y}|}, \tag{15}$$

$$R^2=\frac{\sum_{i=1}^{k}(\hat{y}-\overline{y}_i)^2}{\sum_{i=1}^{k}(y_i-\overline{y}_i)^2}, \tag{16}$$

$$\mathrm{RMAE}=\frac{\max\left\{|y_i-\hat{y}_1|,\cdots,|y_i-\hat{y}_k|\right\}}{\sum_{i=1}^{k}\frac{|y_i-\overline{y}|}{k}}, \tag{17}$$

where k is the number of samples; n is the degree of freedom; the value of n is the number of adjustment parameter minus one; y_i denotes the exact function value at confirmation point i; $\hat{y}_i$ is the corresponding surrogate value; $\overline{y}_i$ is the mean value of y_i. When the value of R^2 and R_{adj}^2 is closer to 1, the fitting precision of the response surface model will be higher.

4.3 Constraint

In general, wrinkling and tearing are major defects except for springback in the three-dimensional stretch bending forming process. High stretch force can result in tearing and reduce wrinkling. The wrinkling in T profiles stretch bending forming is not obvious when the stretch force is adequate. The tearing and wrinkling are considered as the design constraints. Wrinkling and tearing can be represented by forming limit diagram (FLD), but it is difficult to obtain the precise FLD. Wrinkling and tearing are related to the change of the local thickness in the stretch bending forming. Therefore, the changes of the local thickness are used as a criterion of forming limit by many scholars:

$$\Delta t_{\max}=\frac{t_{\max}-t_0}{t_0}, \tag{18}$$

$$\Delta t_{\min}=\frac{t_0-t_{\min}}{t_0}, \tag{19}$$

where $\Delta t_{\max}$ denotes the maximum rate of local thickness change; $\Delta t_{\min}$ represents the minimum rate of local thickness change; and t_0 is the local thickness before forming.

4.4 Procedure for optimization of stretch force trajectory

The particle swarm optimization (PSO) algorithm is widely used and developed rapidly. It is easy to implement and exhibit robust global convergence. It is applied successfully to optimize the design problems of the sheet metal forming process. Sheet metal forming is a nonlinear problem like the profile stretch bending forming process. PSO is chosen to optimize the stretch force trajectories in this paper.

The initial samples are generated by DOE. Assume that the number of samples is n, the response surface is employed to construct the formulation of design optimization problem from n samples. Then we analyze the accuracy of response. If the accuracy of the response surface was acceptable, we optimize the stretch trajectory using PSO for an optimum set of stretch trajectories. Otherwise, it is necessary to add the samples for recalculation. SVR is used to predict the springback and the change of the local thickness of the optimum values. If the springback and change of the local thickness are acceptable, the best stretch trajectory can be obtained. Otherwise, the new samples are needed.

5 Numerical Example

5.1 Optimization of stretch force trajectory

In this paper, the objective optimization for three-dimensional stretch bending for profile is specifically formulated as follows:

$$\begin{aligned}&\min S(x)=f(x),\\ \text{s.t.}\quad &0.02\leqslant g_1(x)\leqslant 0.03,\\ &0\leqslant g_2(x)\leqslant 0.15,\\ &100\,000\ \text{N}\leqslant x_i\leqslant 273\,150\ \text{N},\ 1\leqslant i\leqslant 4,\\ &0.5\%\leqslant x_j\leqslant 1.4\%,\ 1\leqslant j\leqslant 2,\end{aligned}$$

where $g_1(x)$ is denoted as the minimum rate of local thickness change, and $g_2(x)$ represents the maximum rate of local thickness change.

Fifty of the experiments were selected randomly to formulate the response surface model. The accuracy of the response surface was examined. The errors of objective function and constraints were summarized in Table 2. It showed that the response surface model was suitable for the three-dimensional stretch bending forming.

Table 2. Accuracy of response surface

Parameter	RAAE	R^2	RMAE
$S(x)$	0.017 3	0.994 3	0.046 2
$g_1(x)$	0.036 2	0.985 7	0.073 5
$g_2(x)$	0.027 6	0.991 5	0.051 7

After formulating the objective function and constraints, the objective function was optimized by PSO. The parameters of PSO were set as Table 3. The knee point which was found to have the least distance compared with other pareto points was always an overall optimum in the objective space. The value of utopia point is presented in Table 4.

Table 3. Parameters setting of PSO

PSO parameter name	Value
Population size m	100
Personal learning coefficient c_1	1.494
Global learning coefficient c_2	1.494
Inertia weight w	0.729

Table 4. PSO optimal designs

Description	Value
Objective $S(x)$ s/mm	2.037
Constraint $g_1(x)$ $\Delta t_{\min}$	0.024
Constraint $g_2(x)$ $\Delta t_{\max}$	0.082
Variable x_1 f_1/N	159 392
Variable x_2 f_2/N	181 566
Variable x_3 f_3/N	175 426
Variable x_4 f_4/N	167 357
Variable x_5 l_0/%	0.79
Variable x_6 l_1/%	0.85

5.2 Examination on the optimum

In order to examine the optimum of stretch force trajectory, the following four experiments of different stretch force trajectories were tested for the springback reduction in Table 5. The experiment in which variables were set according to the optimum was carried out. The variables of x_1, x_5 and x_6 were applied the optimized values in case 1. The variables of x_2, x_5 and x_6 were used the optimized values in case 2. The variables of x_4, x_5 and x_6 were employed the optimized values in case 3. The variables of x_5 and x_6 were adopted the optimized values in case 4. The variables of x_1, x_2, x_3 and x_4 were employed the optimized values in case 5. The variables were all different from the optimized values in case 6. The comparison of springback and thickness change among the optimum and the four stretch force trajectories were presented in Table 6.

Table 5. Comparison of stretch force trajectories

Case No.	Variable x_1/N	Variable x_2/N	Variable x_3/N	Variable x_4/N	Variable x_5/%	Variable x_6/%
Case 1	159 392	180 257	185 652	181 530	0.79	0.85
Case 2	179 475	181 566	171 789	171 486	0.79	0.85
Case 3	175 580	189 462	178 426	167 357	0.79	0.85
Case 4	159 392	181 566	175 426	167 357	0.72	0.92
Case 5	159 392	181 566	175 426	167 357	0.80	0.88
Case 6	150 348	175 355	165 327	170 217	0.80	0.89

Table 6. Comparison of springback among the optimum and the four stretch force trajectories

Case No.	Springback s/mm	Minimum rate $\Delta t_{\min}$	Maximum rate $\Delta t_{\max}$
Case 1	3.251	0.028	0.135
Case 2	1.852	0.035	0.168
Case 3	2.048	0.027	0.138
Case 4	3.025	0.023	0.076
Case 5	1.803	0.032	0.157
Case 6	3.203	0.026	0.170
Optimum	2.037	0.024	0.082

It can be found that the springback was not the smallest in optimum. The springback in case 2, case 3 and case 5 was lower than that of optimum, but $\Delta t_{\min}$ and $\Delta t_{\max}$ were not acceptable. So case 2 case 3 and case 5 were not the best parameters. The value of springback of optimum was lower than case 1, case 4 and case 6, simultaneously the values of $\Delta t_{\min}$ and $\Delta t_{\max}$ were acceptable. The value of springback of optimum in experiment was close to the value in the response surface model. It can be suggested that the stretch force trajectory during the three-dimensional stretch bending played an important role for the springback reduction.

6 Conclusions

(1) According to the characteristics of the three-dimensional stretch bending process, the flexible die is presented, which can be reconfigurable for the target shape of profile, and the constructive method of the die face is carried out.

(2) Springback prediction based on SVR is proposed which has higher accuracy than ANN. The input parameters of SVR are variable stretch force trajectories.

(3) The fitting function of springback in three-dimensional stretch bending process using response surface is suitable.

(4) The stretch force trajectory in three-dimensional stretch bending is optimized by PSO algorithm. The optimized stretch force trajectory is proved to efficiently reduce the springback.

References

[1] PAULSEN Frode, WELO Torgeir. Cross-sectional deformations of rectangular hollow in bending: Part I-experiments[J]. *International Journal of Mechanical Science*, 2003, 43: 109–129.

[2] PAULSEN Frode, WELO Torgeir. Cross-sectional deformations of rectangular hollow in bending: Part Ⅱ-analytical models[J]. *International Journal of Mechanical Science*, 2003, 43: 131–152.

[3] LIANG Jicai, TENG Fei, GAO Song, et al. Key technologies research on the forming process of flexible three-dimensional stretch bending[J]. *Journal of Mechanical Engineering*, 2013, 49(17): 187–192. (in Chinese)

[4] LIANG Jicai, GAO Song, TENG Fei, et al. Flexible 3D stretch-bending technology for aluminum profile[J]. *International Journal of Advanced Manufacturing Technology*, 2014, 71: 1939–1947.

[5] SRINIVASAN R, VASUDEVAN D, PADMANABHAN P. Influence of friction parameters on springback and bend force in air bending of electrogalvanised steel sheet: an experimental study[J]. *Journal of Brazilin Society of Mechanical Sciences and Engineering*, 2013, 36: 371–376.

[6] CHOI K Y, LEE M G, KIM H Y. Sheet metal forming simulation considering die deformation[J]. *International Journal of Automotive Technology*, 2013, 14(6): 935–940.

[7] RAJU S, GANESAN G, KARTHIKEYAN R. Sensitivity analysis and statistical process optimization of deep drawing of AA6061 sheet material[J]. *Materials Science and Technology*, 2013, 29(5): 573–580.

[8] FIRAT Mehmet, KARADENIZ Erdal, YENICE Mustafa, et al. Improving the accuracy of stamping analyses including springback deformations[J]. *Journal of Material Engineering and Performance*, 2013, 22(2): 332–337.

[9] MILLER J E, KYRIAKODES S, BASTARD A H. On bend-stretch forming of aluminum extruded tubes-Ⅰ: experiments[J]. *International Journal of Mechanical Sciences*, 2001, 43: 1283–1317.

[10] MILLER J E, KYRIAKODES S, CORONA E. On bend-stretch forming of aluminum extruded tubes-Ⅱ: analysis[J]. *International Journal of Mechanical Sciences*, 2001, 43: 1319–1338.

[11] CLAUSEN Arild H, HOPPERSTAD Odd S, LANGSETH Magnus. Sensitivity of model parameters in stretch bending of aluminum

extrusions[J]. *International Journal of Mechanical Sciences*, 2001, 43: 427–453.

[12] YU Zhongqi, LIN Zhongqin. Numerical analysis of dimension precision of U-shaped aluminium profile rotary stretch bending[J]. *Transactions of Nonferrous Metals Society of China*, 2007, 17: 581–585.

[13] LIANG Jicai, TENG Fei, GAO Song, et al. Multi-objective optimization of flexible three-dimensional stretch-bending forming process of rectangular hollow aluminum profiles[J]. *Journal of South China University of Technology (National Science Edition)*, 2013, 41(9): 143–148. (in Chinese)

[14] LEE SW, KIM YT. A study on springback in the sheet metal flag drawing[J]. *Journal Mater Process Technol.*, 2007, 187: 89–93.

[15] OUAKDI E H, LOUAHDI R, KHIRANI D, et al. Evaluation of springback under the effect of holding force and die radius in a stretch bending test[J]. *Materials and Design*, 2012, 35: 106–112.

[16] CAO J, KINSEY B, SOLLA SA. Consistent and minimal springback using a stepped binder force trajectory and neural network control[J]. *Journal of Engineering Materials and Technology*, 2000, 122: 113–118.

[17] KITAYAMA Satoshi, HUANG Suisheng, YAMAZAKI Koetsu. Optimization of variable blank holder force trajectory for springback reduction via sequential approximate optimization with radial basis function network[J]. *Structural Multidisciplinary Optimization*, 2013, 47: 289–300.

[18] KITAYAMA Satoshi, YOSHIOKA Hiroki. Springback reduction with control of punch speed and blank holder force via sequential approximate optimization with radial basis function network[J]. *International Journal of Mechanics and Materials in Design*, 2014, 10: 109–119.

[19] KAZAN R Kazan, FIRAT M, TIRYAKI A E. Prediction of springback in wipe-bending process of sheet metal using neural networks[J]. *Materials and Design*, 2009, 30(2): 418–423.

[20] SONG Y, YU Z. Springback prediction in T-section beam bending process using neural networks and finite element method[J]. *Archive of Civil and Mechanical Engineering*, 2013, 3: 229–241.

[21] HONG W C, PAI P F. Predicting engine reliability by support vector machine[J]. *International Journal of Advanced Manufacturing Technology*, 2006, 28: 154–161.

[22] SINGH Swadensh Kumar, GUPTA Amit Kumar. Application of support vector regression in predicting thickness strains in hydro-mechanical deep drawing and comparison with ANN and FEM[J]. *CIRP Journal of Manufacturing Science and Technology*, 2010, 3: 66–72.

[23] SCHOLKOPF B, SMOLA A J. *Learning with kernel: support vector machines, regularization, optimization, and beyond*[M]. Cambridge: MIT, 2002.

Biographical notes

TENG Fei, born in 1985, is currently a PhD candidate at *Automotive Engineering Institute, Dalian University of Technology, China*. She received her master bachelor degree from *Jilin University, China*, in 2011. Her research interests include auto materials processing.
Tel: +86-18584367161; E-mail: tengfei325@126.com

ZHANG Wanxi, born in 1954, is currently a professor at *Dalian University of Technology, China*. He received his master degree from *Changchun Institute of Applied Chemistry*, *China*, in 1982.
E-mail: zhangwanxi0626@sina.com

LIANG Jicai, born in 1958, is currently a professor at *Jilin University, China*, in 2001. His research interests include auto materials processing.
E-mail: liangjicai@126.com

GAO Song, born in 1987, is currently a PhD candidate at *Automotive Engineering Institute, Dalian University of Technology, China*. His research interests include auto materials processing.
E-mail: gaosong@126.com